Advantages of a new approach for estimating the stator resistance of a permanent magnet synchronous machine compared to known conventional methods

Sven Ludwig Kellner and Bernhard Piepenbreier
Friedrich-Alexander-University Erlangen-Nuremberg, Chair of Electrical Drives and Machines, Erlangen, Germany
Kellner@eam.eei.uni-erlangen.de

***Abstract*—Usually, electrical propulsion vehicles are driven by highly dynamic drive controls. To make this possible, it is important to know electrical parameters such as inductances, flux and stator resistance as exactly as possible. In particular, the ohmic stator resistance R_s changes during operation due to temperature changes. Therefore, it is not possible to achieve a high precision over a wide operating temperature range with an offline measurement of R_s. In this paper, a new identification method for stator resistance is presented and compared to a known method. While the conventional method only works properly at certain operating points, the new method does not have this limitation.**

***Index Terms*—adjustable speed drive, control of drive, drive, electrical drive, electrical machine, permanent magnet motor, variable speed drive**

I. Introduction

Traction drives, especially, require highly utilized electric machines. This paper is restricted to drive systems using permanent magnet synchronous machines (PMSM). To control these drive systems, the field-orientated approach is widely accepted. The electrical parameters that are needed are the ohmic stator resistance R_s, permanent magnet flux ψ_p and stator inductances L_d and L_q, where d and q correspond to the axes of the rotor fixed coordinate system [1], as shown in Fig. 1. If R_s and L are not known accurately, ψ_p and consequently the torque T cannot be calculated well enough. As the torque is not measured in most cases although it is needed for the field-oriented control approach, nevertheless an exact calculation of the instantaneous torque needs to be made as a function of the machine parameters. According to conventional methods, the ohmic stator resistance R_s can be measured accurately at standstill when a high load is applied. Especially in automotive applications, this state does not occur very often. More often, the drive is at standstill with no load or is running at medium speed with medium load, for example. As shown in this paper, in these states, the measurement of R_s by conventional methods is impossible.

To solve this problem a large variety of methods is known. A model reference adaptive system (MRAS) technique for estimating the electrical parameters is chosen in [2] for instance. Apart from this, different types of parameter identification methods are known. Reference [3], for example, uses a current test signal with different amplitudes on the d- and q-axes. As this method requires an exact knowledge of ψ_p, it is not applicable under most circumstances. Also, the method has only been proven by simulation. Another approach is based on high frequency signal injection. In the associated publication [4], no kind of simulation or measurement results for the identified stator resistance R_s are shown. Reference [5] describes an identification method for stator resistance which is unstable. An approach only suitable for sensorless controlled machines is shown in [6]. This method calculates the stator resistance using the actual speed estimation error as a co-product of the HF signal needed for sensorless controlled drives at near zero speed.

Contrary to [4] and [6], the new approach for identifying the ohmic stator resistance R_s presented in this paper uses low frequency current signal injection on the d-axis. Its frequency is about 2 Hz. The identification algorithm has to be calculated once during every half wave of the test signal. When a 2 Hz test signal frequency is used, the calculation is only done four times a second. This results in a small amount of computation time being used. Besides this, the proposed method has two further significant advantages: First, when reluctance effects are ignored, the output torque of the PMSM remains unchanged. Second, the temperature dependency, and thus the often inaccurately known electrical parameter ψ_p are not needed in the identification equations.

II. PMSM Model

The general voltage phasor for a PMSM in the complex d,q-coordinate system according to Fig. 1 can be written as:

$$\underline{u}^{d,q} = R_s \, \underline{i}^{d,q} + \frac{d}{dt} \, \underline{\psi}^{d,q} + \mathrm{j} \, \omega_{el} \, \underline{\psi}^{d,q} \; . \qquad (1)$$

The basic idea of the field-oriented control approach is to separately control the d- and q-axes, so it is convenient to split the complex voltage phasor (1) into the two equations (2) and (3). Together with a third equation (4) for the internal torque T_i of the PMSM, they describe the behavior of the PMSM in

978-1-4244-8218-4/10/$26.00

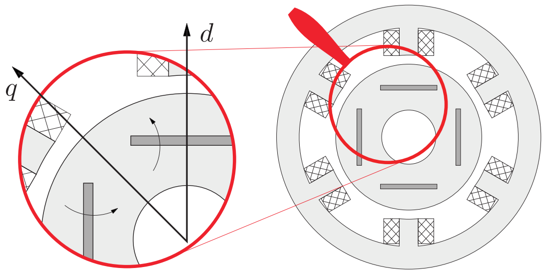

Fig. 1. Definition of the complex d,q-coordinate system for a permanent magnet synchronous machine with internal magnets.

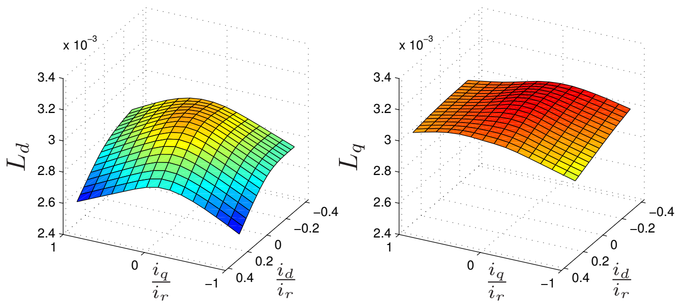

(a) L_d in H (b) L_q in H

Fig. 2. Measured inductances $L_d^{(i_d,i_q)}$ and $L_q^{(i_d,i_q)}$ of the PMSM with surface-mounted permanent magnets used in test bench 2. All currents are based on rated values (r).

d,q-coordinates.

$$u_d = R_s\, i_d + \frac{d}{dt}\; \psi_d - \omega_{el}\, \psi_q \tag{2}$$

$$u_q = R_s\, i_q + \frac{d}{dt}\; \psi_q + \omega_{el}\, \psi_d \tag{3}$$

$$T_i = \frac{3}{2}\, \frac{p}{\omega_{el}} \left(\frac{d\,\psi_d}{d\,t} - \omega_{el}\, \psi_q\, i_d + \frac{d\,\psi_q}{d\,t} + \omega_{el}\, \psi_d\, i_q \right) \,. \tag{4}$$

It has to be assumed that the electrical parameters of the machine such as changes to inductances during normal operation depend on the currents i_d and i_q, respectively. Then, the flux linkages ψ_d and ψ_q can in general be written as:

$$\psi_d = \psi_p + L_d^{(i_d,i_q)} \cdot i_d \quad \text{and} \tag{5}$$

$$\psi_q = L_q^{(i_d,i_q)} \cdot i_q \;. \tag{6}$$

When cross coupling effects are neglected, the voltage equations (2) and (3) can be rewritten as:

$$u_d = R_s\, i_d + L_{dd}^{(i_d,i_q)}\, \frac{d\,i_d}{d\,t} - \omega_{el}\, L_q^{(i_d,i_q)}\, i_q \quad \text{and} \tag{7}$$

$$u_q = R_s\, i_q + L_{qq}^{(i_d,i_q)}\, \frac{d\,i_q}{d\,t} + \omega_{el}\, L_d^{(i_d,i_q)}\, i_d + \omega_{el}\, \psi_p \;. \tag{8}$$

$L_d^{(i_d,i_q)}$ and $L_q^{(i_d,i_q)}$ represent the absolute inductances. The superscript (i_d, i_q) indicates that the inductances are dependent on i_d and i_q. $L_{dd}^{(i_d,i_q)}$ and $L_{qq}^{(i_d,i_q)}$ represent the differential inductances of the machine in the d,q-coordinate system. They are abbreviations of the terms

$$L_{dd}^{(i_d,i_q)} = \left. \frac{\partial\, \psi_d(i_d, i_q)}{\partial\, i_d} \right|_{i_d,i_q} \quad \text{and} \tag{9}$$

$$L_{qq}^{(i_d,i_q)} = \left. \frac{\partial\, \psi_q(i_d, i_q)}{\partial\, i_q} \right|_{i_d,i_q} \;. \tag{10}$$

Fig. 2 shows examples of curves for the inductances $L_d^{(i_d,i_q)}$ and $L_q^{(i_d,i_q)}$. They are the measured inductances of the PMSM with surface-mounted permanent magnets used in test bench 2. It can be seen that the inductances shown vary significantly with changing i_d and i_q, respectively.

The internal torque T_i can also be rewritten with (5) and (6) inserted into (4). As before, cross coupling effects are neglected in this equation:

$$T_i = \frac{3}{2}\, \frac{p}{\omega_{el}} \left(L_{dd}^{(i_d,i_q)}\, \frac{d\,i_q}{d\,t} + L_{qq}^{(i_d,i_q)}\, \frac{d\,i_d}{d\,t} + \omega_{el} \left(L_d^{(i_d,i_q)} - L_q^{(i_d,i_q)} \right) i_d\, i_q + \omega_{el}\, \psi_p\, i_q \right) \,. \tag{11}$$

Field-orientated control of high dynamic drive applications requires as accurate a knowledge as possible of the electrical parameters ψ_p and R_s, whereas they remain unknown in (7) and (8). Therefore an adequate identification of R_s is needed; two methods are described in this paper.

III. Conventional Method

An easy way to get the stator resistance R_s is to neglect all derivatives of the currents (stationary state) and solve (8) accordingly:

$$R_{s,conv,1} = \frac{u_q - \omega_{el}\, L_d^{(i_d,i_q)}\, i_d - \omega_{el}\, \psi_p}{i_q} \;. \tag{12}$$

The problem with (12) is that, in most cases, the permanent magnet flux ψ_p is normally only known approximately. This is because the flux ψ_p of permanent magnets is dependent on the rotor temperature which is normally not measured on permanent magnet synchronous machines [7] [8]. With the wrong ψ_p, a speed-dependent measurement error is introduced into (12). In addition, there is always a current i_q and therefore a non-zero torque that is needed to evaluate (12).

The method described in (12) can be slightly optimized by using a model-based system [9]. In general, the measurement algorithm does not have the ideal values. At least ψ_p and consequently u_q are in error. So one can define two equations. One equation assuming all parameters are well known:

$$u_q = R_s\, i_q + \omega_{el}\, L_d^{(i_d,i_q)}\, i_d + \omega_{el}\, \psi_p \;, \tag{13}$$

and another with the erroneous values

$$\hat{u}_q = \hat{R}_s\, i_q + \omega_{el}\, L_d^{(i_d,i_q)}\, i_d + \omega_{el}\, \hat{\psi}_p \;. \tag{14}$$

The stator resistance error $\Delta R_{s,conv,2} = R_s - \hat{R}_s$ can then be written as

$$\Delta R_{s,conv,2} = \frac{\Delta u_q + \omega_{el}\,\Delta\psi_p}{i_q} = \frac{\Delta u_q}{i_q} + \frac{\omega_{el}\,\Delta\psi_p}{i_q} \ . \quad (15)$$

The voltage error $\Delta u_q = u_q - \hat{u}_q$ is well known. As described previously, the flux ψ_p and therefore the flux error $\Delta\psi_q = \psi_q - \hat{\psi}_q$ is not equal to zero in many cases. Despite this, (15) is an improvement on (12), because neither $L_d^{(i_d,i_q)}$ nor i_d are required in (15) if the assumption is made that $L_d^{(i_d,i_q)}$ is sufficiently well known, e.g. by offline measurement whith results shown in Fig. 2.

The main disadvantages of the conventional methods (12) and (15) for measuring R_s are obvious. If a non-zero speed error is present, any error in ψ_p amplifies the error in R_s. As i_q is in the denominator of (12) and (15), this error gets even bigger if i_q and therefore the load torque is small.

Thus, the conventional measurement methods without any test signals are only suitable at relatively high load conditions together with near zero speed of the electrical drive system.

IV. Novel identification theory

As shown, the simple conventional methods for measuring R_s online only work at certain operating points. The proposed algorithm was designed to take minimal computational time and to be as robust and accurate as possible. The entire identification process runs within the d,q-coordinate system. In general, there are two options: As a basis for identification, the u_d-equation (7) or u_q-equation (8) can be used. As both depend on R_s, basically the identification of resistance R_s is possible with both equations. However, (8) is not suitable for the proposed algorithm for two reasons: First, at least under no load conditions, an alternating test current i_q would be necessary. This would cause an intolerable amount of oscillating torque. Second, (8) also depends on the permanent magnet flux linkage ψ_p which is not known with sufficient accuracy. So, (7) is taken as the basis of the identification algorithm. The influence of an alternating current i_d due to cross-coupling effects is very low. In addition, there is no ψ_p in (7) and therefore it does not need to be known.

The new approach is based on the assumption that a high proportion of the measurement errors are offset errors. So an alternating test signal current i_d creates two time instants. When the two generated u_d-equations are subtracted from one another, the offset errors are minimized. Errors depending on speed and measurement noise are minimized before using an appropriate filtering method which is described later on.

The time instants needed are named $^{(1)}$ and $^{(2)}$. Equation (7) would then lead to the two equations

$$u_d^{(1)} = R_s\, i_d^{(1)} + L_{dd}^{(i_d^{(1)},i_q^{(1)})}\,\frac{d\,i_d^{(1)}}{d\,t} - \omega_{el}^{(1)}\,L_q^{(i_d^{(1)},i_q^{(1)})}\,i_q^{(1)} \quad (16)$$

$$u_d^{(2)} = R_s\, i_d^{(2)} + L_{dd}^{(i_d^{(2)},i_q^{(2)})}\,\frac{d\,i_d^{(2)}}{d\,t} - \omega_{el}^{(2)}\,L_q^{(i_d^{(2)},i_q^{(2)})}\,i_q^{(2)} \ . \quad (17)$$

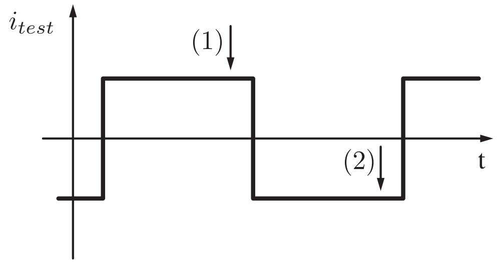

Fig. 3. Test signal current on d-axis. The two points 1 and 2 mark the states introduced in (16) and (17) during the identification process.

Rearranged, (16) and (17) lead to

$$\begin{aligned} u_d^{(2)} - u_d^{(1)} &= R_s\left(i_d^{(2)} - i_d^{(1)}\right) + L_{dd}^{(i_d^{(2)},i_q^{(2)})}\,\frac{d\,i_d^{(2)}}{d\,t} \\ &- L_{dd}^{(i_d^{(1)},i_q^{(1)})}\,\frac{d\,i_d^{(1)}}{d\,t} - \omega_{el}^{(2)}\,L_q^{(i_d^{(2)},i_q^{(2)})}\,i_q^{(2)} \\ &+ \omega_{el}^{(1)}\,L_q^{(i_d^{(1)},i_q^{(1)})}\,i_q^{(1)} \ . \end{aligned} \quad (18)$$

The test current i_d does not change during the measurement of the two time instants. This is realized by using a rectangular test current according to Fig. 3. A constant i_d leads to

$$\frac{d\,i_d^{(1)}}{d\,t} = \frac{d\,i_d^{(2)}}{d\,t} \overset{!}{=} 0 \ . \quad (19)$$

So $L_{dd}^{(i_d,i_q)}$ does not need to be known. The test signal frequency is about 2 Hz. Taking into account the fact that traction drives usually have high inertia, one can assume that the speed of the traction drive does not change very much during a test signal period and therefore

$$\omega_{el}^{(1)} = \omega_{el}^{(2)} \ . \quad (20)$$

Then, (18) can be simplified to

$$\begin{aligned} u_d^{(2)} - u_d^{(1)} &= R_s\left(i_d^{(2)} - i_d^{(1)}\right) \\ &- \omega_{el}\left(L_q^{(i_d^{(2)},i_q^{(2)})}\,i_q^{(2)} + L_q^{(i_d^{(1)},i_q^{(1)})}\,i_q^{(1)}\right) \ . \end{aligned} \quad (21)$$

So, the identification equation according to the proposed method results in:

$$\begin{aligned} R_{s,ident} &\overset{!}{=} \frac{1}{i_d^{(2)} - i_d^{(1)}} \cdot \Bigg[u_d^{(2)} - u_d^{(1)} \\ &+ \omega_{el}\left(L_q^{(i_d^{(2)},i_q^{(2)})}\,i_q^{(2)} - L_q^{(i_d^{(1)},i_q^{(1)})}\,i_q^{(1)}\right)\Bigg] \ . \end{aligned} \quad (22)$$

It can be seen that under standstill conditions, only u_d and i_d are relevant variables. In addition: the higher the test current amplitudes, the better the R_s-identification.

The main source of uncertainty in (22) is the inductance $L_q^{(i_d,i_q)}$, even when it is measured in advance. However, this source of error is reduced due to the subtraction of the two time instants. When not only the drive speed but also the

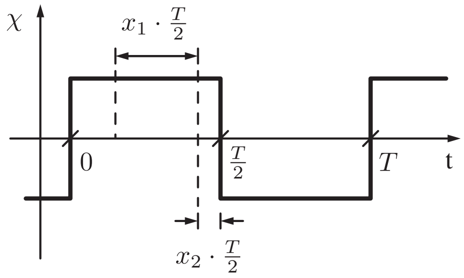

Fig. 4. Filtering of measurement signals.

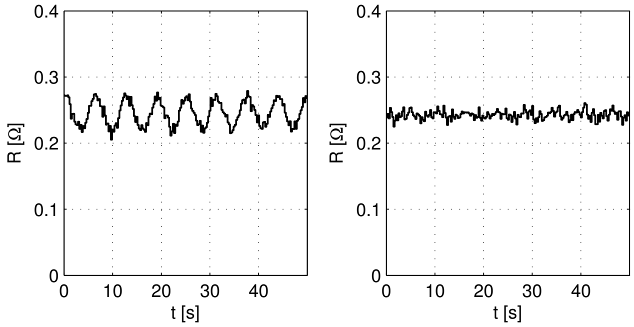

(a) t_f = const. (b) t_f = variable

Fig. 5. Identification results of R_s by filtering with constant (a) and variable (b) filtering window of IPMSM (test bench 1). The speed variable filtering method (b) does not show low frequency harmonics in the identification results in contrast to (a).

i_q current is constant within a test signal period, the speed-dependent term of (22) simplifies to:

$$\omega_{el}\, i_q \left(L_q^{(i_d^{(2)}, i_q)} - L_q^{(i_d^{(1)}, i_q)} \right) \quad . \tag{23}$$

Especially when $i_d \approx 0$, the change in $L_q^{(i_d,i_q)}$ is rather small and therefore the measurement errors of $L_q^{(i_d,i_q)}$ do not have much influence on the identification result.

Due to various effects, the measurement signals are overlaid by the 6th harmonic of the speed [10]. To eliminate this harmonic, the measurement signals should be adequately filtered.

The new filtering method selects an adequate period of time within one rectangular half cycle of the test signal period. It integrates the noisy measurement signals $\chi(t)$ over this period and uses the mean value:

$$\frac{2}{x_1 T} \int_{\frac{T}{2}(1-x_1-x_2)}^{\frac{T}{2}(1-x_2)} \chi(t)\; dt \; . \tag{24}$$

Fig. 4 explains the filtering process in a more illustrative way. The length of the filtering window is adjusted by x_1, the distance to the next rectangular half cycle of the test signal current by x_2.

When the filtering duration $t_f = x_1 \frac{T}{2}$ is constant, there will be a speed-dependent beat in the filtered measured signals because of the 6th harmonic already described, since the filtering duration t_f is not an integer multiple of the 6th harmonic. This is why the filtering duration t_f is adapted by means of the parameter $x_1(\omega_{el})$. This eliminates the low frequency beat. Fig. 5 shows the difference between a constant t_f (a) and a speed-dependent t_f (b). Fig. 5a is overlaid with a low frequency beat. As this beat can have a cycle time of 30 seconds and more, it prevents an exact identification of R_s and therefore it is most important to eliminate it. Measurements covering the entire operating range were made. Due to this new filtering method, the beat was effectively

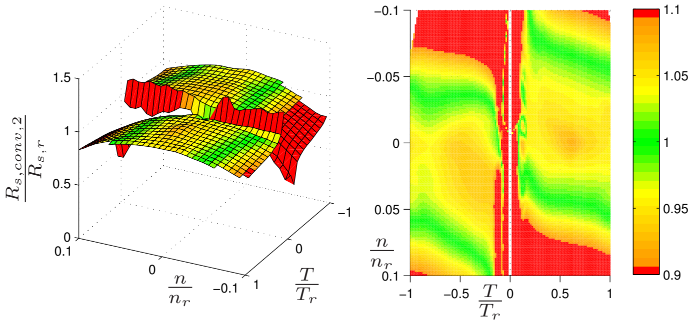

(a) 3D view (b) 2D view

Fig. 6. Test bench 1: Measurement of R_s by **conventional method** according to (15) and $\psi_p = \psi_{p,real}$. No measurement of R_s is possible at no load ($T \approx 0$). At higher speed, the measurement gets significantly worse.

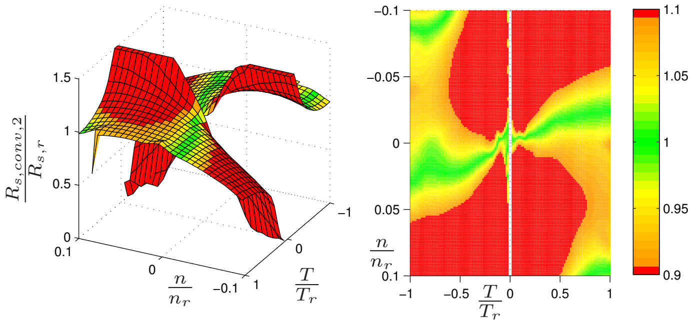

(a) 3D view (b) 2D view

Fig. 7. Test bench 1: Measurement of R_s by **conventional method** according to (15) and $\psi_p = 0,9\, \psi_{p,real}$. With no exact permanent magnet flux known, the measurement gets considerably worse compared to Fig. 6.

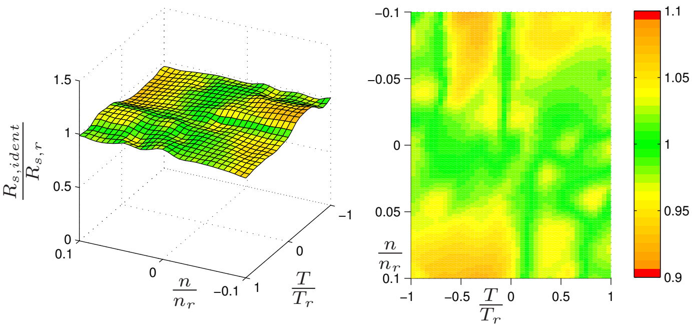

(a) 3D view (b) 2D view

Fig. 8. Test bench 1: Measurement of R_s by **new identification method** according to (22). Contrary to the conventional method, the error is always less than 10% and identification is also possible at zero load ($T = 0$)

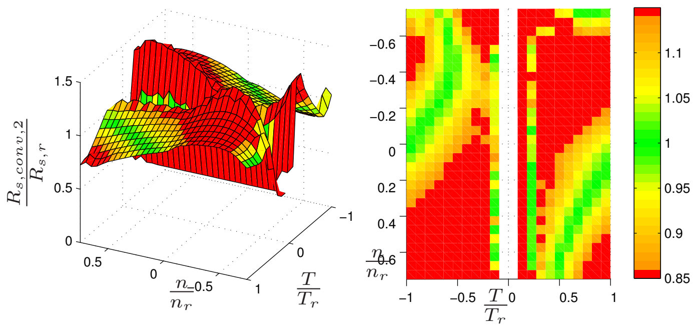

(a) 3D view (b) 2D view

Fig. 9. Test bench 2: Measurement of R_s by **conventional method** according to (15) and $\psi_p \approx \psi_{p,real}$. The only reliable operating point exists at zero speed and rated load.

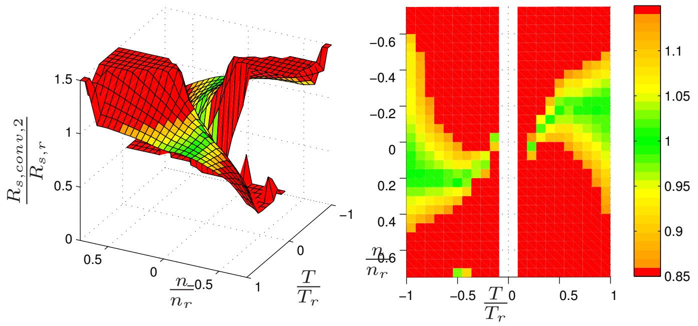

(a) 3D view (b) 2D view

Fig. 10. Test bench 2: Measurement of R_s by **conventional method** according to (15) and $\psi_p \approx 0.98\,\psi_{p,real}$. With no exact permanent magnet flux known, the measurement gets considerably worse compared to Fig. 9.

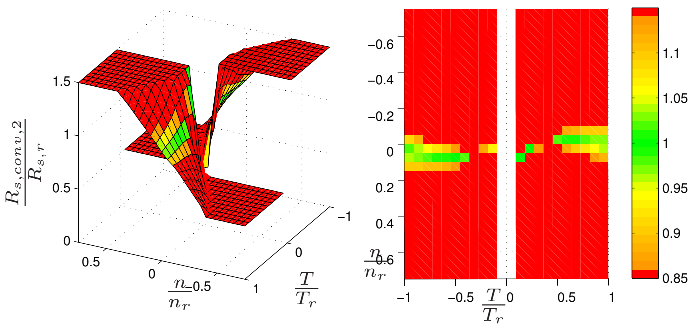

(a) 3D view (b) 2D view

Fig. 11. Test bench 2: Measurement of R_s by **conventional method** according to (15) and $\psi_p = 0.95\psi_{p,real}$. No measurement of R_s is possible with no load ($T \approx 0$).

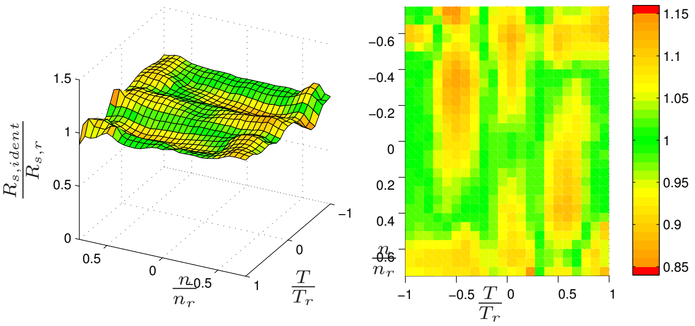

(a) 3D view (b) 2D view

Fig. 12. Test bench 2: Measurement of R_s by **new identification method** according to (22). In contrast with the conventional method, the error is always less than 15 % and identification is also possible at zero load ($T = 0$).

eliminated where present.

A further advantage of this filtering method lies in the considerably reduced computing time compared to other filtering methods, because only one register is needed for the integration process. The use of a sliding average method, for example, would require one register per averaging step and thereby need a lot more computation time.

V. Error Analysis

For a function $y = f(x_1, x_2, \ldots, x_n)$, the input errors δx_i are related to the output errors δy by:

$$\delta y = \sum_{i=1}^{n} \left| \frac{\partial}{\partial x_i} f(x_1, x_2, \ldots, x_n) \right| \delta x_i \ . \tag{25}$$

To simplify the calculation, only a permanent magnet flux error $\delta\psi$ and voltage error δu are considered. The flux is dependent on the unknown rotor temperature. The voltages u_d and u_q can only be calculated via the duty cycle of the converter. As the converter does not have exactly known non-linearities, even linearized voltages have a relevant error.

Based on (25), the error in the conventional method from (15) is

$$\delta R_{s,conv,2} = \frac{1}{|i_q|} \cdot \delta u_q + \left| \frac{\omega_{el}}{i_q} \right| \cdot \delta\psi_p \ , \tag{26}$$

whereas the identification error in the new method is

$$\delta R_{s,ident} = \frac{\delta u_d^{(2)} + \delta u_d^{(1)}}{\left| i_d^{(2)} - i_d^{(1)} \right|} \ . \tag{27}$$

One can easily see that in (26) the error depends on i_q and ω_{el}. These values change during operation. In contrast, the new algorithm (27) has an error that is only dependent on the amplitude of the low frequency test signal and therefore does not change during operation. If the errors of $u_d^{(1)}$ and $u_d^{(2)}$ are offset errors with the same algebraic sign, then according to (27) the two errors cancel out each other.

VI. Test Bench 1

Both methods, the conventional method according to (15) and the new identification method according to (22), were implemented on a test bench with an internal permanent magnet synchronous machine (IPMSM) with a rated output power of 22 kW and armature windings consisting of concentrated coils. The IPMSM generated extensive harmonics. Along with the limited PWM inverter switching frequency of 2 kHz, the maximum speed for test bench 1 was as low as $n = 0.1 \cdot n_{rated} = 150\,\frac{1}{\text{min}}$.

Figures 6 and 7 show the measurement results obtained with by conventional method. The surfaces shown are constructed from 169 stationary state operating points which were uniformly distributed over the operating range to cover all possible speed and torque combinations. To make the figure more understandable, the identification results were scaled by the real ohmic stator resistance which is calculated from an offline reference value of $R_{s,20^{\circ}\mathrm{C}}$ combined with the actual measured stator temperature. For example, a value of 1.1 in Fig. 6 represents an identification error of $10\,\%$.

In Fig. 6, the permanent magnet flux ψ_p in (15) was known as exactly as possible, in the second one it is assumed to be $10\,\%$ lower. The latter simulates an imperfectly known flux ψ_p, e.g. caused by temperature changes of the rotor magnets. It can be seen, that the conventional method has a significant dependency on the flux ψ_p. If this is not known accurately, as shown in Fig. 7 for example, the measurement of R_s is almost impossible, the relative errors can readily exceed the real value of R_s by much more than 10 %. Especially at non-zero speeds, the conventional approach is of no use. In addition, at near zero load, no measurement is possible, even when ψ_p is known exactly.

In contrast, Fig. 8 shows the identification of R_s according to the new identification method. Over the entire measuring range, the identification error is less than $\pm 10\,\%$ of the real value of R_s. Apart from this, identification is also possible at zero load with no limitations.

VII. Test bench 2

In addition, the two methods are compared on a second test bench with a PMSM with surface-mounted permanent magnets and a rated output power of 26 kW. Contrary to test bench 1, higher speeds up to $n = 1500 \frac{1}{\text{min}} = 0.75 \cdot n_{rated}$ are possible on test bench 2. The maximum speed was limited by test bench limitations, not because of identification issues.

Figures 9, 10 and 11 show the identification results obtained with the conventional method by measuring R_s according to Eq. (15). As on test bench 1, the speed and torque were held constant at each operating point. The identified ohmic stator resistance was scaled by the real value. It can be seen that even small changes in the permanent magnet flux ψ_p have a significant effect on the R_s calculation. This is why even in Fig. 9 when ψ_p is assumed to be known as ideally as possible, the result obtained by the conventional method is only accurate at high load under standstill conditions. Figures 10 and 11 show the results from the conventional method when the wrong ψ_p is assumed: By 2 % and 5 %, respectively. The error is considerably higher than in Fig. 9 where $\psi_p \approx \psi_{p,real}$.

The new identification method is shown in Fig. 12. In contrast with the conventional measurement results, the maximum error over the whole operating range is limited to $\pm 15\,\%$. In addition, identification is possible under conditions with no load.

VIII. Conclusion

For traction drives especially, drive control has to be simultaneously dynamic and accurate. Therefore, knowledge of the highly temperature-dependent ohmic stator resistance R_s is relevant. In this paper, a new approach for identifying the ohmic stator resistance R_s online with low frequency test signals is compared to a conventional method. The limitations of the conventional method are shown, especially under conditions of no load and non-zero speed when measurements are almost impossible by the conventional method.

In contrast, the new identification method is insensitive to input parameter errors and the permanent magnet flux is not needed for the identification process. The new method is not limited to any special speed or load operating point.

References

[1] P. Vas, *Vector control of AC machines*. Oxford: Clarendon Press, 1994.

[2] K.-H. Kim, S.-K. Chung, G.-W. Moon, I.-C. Baik, and M.-J. Youn, "Parameter estimation and control for permanent magnet synchronous motor drive using model reference adaptive technique," *International Conference on Industrial Electronics, Control, and Instrumentation (IECON)*, vol. 21, pp. 387–392, 1995.

[3] S. D. Wilson, G. W. Jewell, and P. G. Stewart, "Resistance estimation for temperature determination in pmsms through signal injection," *International Conference on Electric Machines and Drives*, pp. 735–740, 2005.

[4] K.-W. Lee, D.-H. Jung, and I.-J. Ha, "An online identification method for both stator resistance and back-emf coefficient of pmsms without rotational transducers," *IEEE Transactions on Industrial Electronics*, vol. 51, no. 2, pp. 507–510, 2004.

[5] S. Ichikawa, M. Tomita, S. Doki, and S. Okuma, "Sensorless control of permanent-magnet synchronous motors using online parameter identification based on system identification theory," *IEEE Transactions on Industrial Electronics*, vol. 53, no. 2, pp. 363–372, 2006.

[6] A. Piippo, "Stator resistance adaption in sensorless pmsm drives," Patent EP 1 986 317 A1, 29.10.2008.

[7] P. Campbell, *Permanent magnet materials and their application*, 1st ed. Cambridge: Cambridge University Press, 1996.

[8] E. P. Furlani, *Permanent magnet and electromechanical devices - Materials, analysis, and applications*, ser. Series in electromagnetism. San Diego, California: Acad. Press, 2001.

[9] T. Frenzke, *Geberlose Drehmoment-Regelung für permanentmagneterregte Synchronmaschinen in der Bahntraktion: Univ., Diss.–Erlangen-Nürnberg, 2007.*, ser. Berichte aus der Elektrotechnik. Aachen: Shaker, 2008.

[10] I. Hahn, "Einfluss der höheren harmonischen der induzierten spannung auf das betriebsverhalten von motoren mit konzentrierten wicklungen," *VDI-Tagung für Elektrisch-mechanische Antriebssysteme Fulda*, pp. 235–252, 2004.